Electronic Supplementary Information

Symmetry breaking phase transition-triggered high-temperature solid-state quadratic nonlinear optical switch coupled with switchable dielectric constant in an organic–inorganic hybrid compound

Guang-Quan Mei,[*a] Han-Yue Zhang[b] and Wei-Qiang Liao[c]

[a]Key Laboratory of Jiangxi University for Applied Chemistry and Chemical Biology, Yichun University, Yichun 336000, China. E-mail: yc_mgq@163.com

[b]School of Chemistry and Materials Science, Nanjing Normal University, Nanjing, 210023, JiangSu, P. R. China.

[c]Ordered Matter Science Research Center, Southeast University, Nanjing 211189, PR China.

Experimental details

Synthetic procedures. Single crystals of $[NH_3(CH_2)_5NH_3]SbCl_5$ were prepared by slow evaporation of a hydrochloric acid solution containing stoichiometric amounts of 1,5-pentanediamine and $SbCl_3$ at room temperature. In the infrared (IR) spectra of **1** (Fig. S3), the two bands observed at 3201 and 3129 cm^{-1} were assigned to the NH_3 asymmetric stretching vibrations. The CH_2 asymmetric stretching mode can be observed at 2923 cm^{-1}. The powder X-ray diffraction (PXRD) patterns match well with the simulated ones based on the crystal structures for different phases (Fig. S4), confirming the phase purity of the as-grown crystals.

Single-crystal X-ray crystallography. Variable-temperature X-ray single-crystal diffraction data at 293 and 393 K were collected on a Rigaku Saturn 924 diffractometer with Mo–Kα radiation (λ = 0.71073 Å). The Crystalclear software

package (Rigaku, 2005) was used for data processing including empirical absorption corrections. The structures were solved by direct methods and refined by the full-matrix method based on F^2 using the SHELXLTL software package. All non-hydrogen atoms were refined anisotropically using all reflections with $I > 2\sigma(I)$. The positions of the hydrogen atoms were generated geometrically and refined using a "riding" model with $U_{iso} = 1.2U_{eq}$ (C and N). The molecular structures and the packing views were drawn with DIAMOND (Brandenburg and Putz, 2005). Angles and distances between some atoms were carried out using DIAMOND, and other calculations were calculated using SHELXLTL. Crystallographic data and structure refinement at 293 and 393 K are listed in Table S1.

Physical measurements IR spectra were recorded at ambient temperature using a Shimadzu model IR-60 spectrometer with KBr pellets. PXRD was measured on a Rigaku D/MAX 2000 PC X-ray diffraction Instrument at selected temperatures. The simulated powder diffraction patterns were calculated with the Mercury 3.1 program from the Cambridge Crystallographic Data Centre, using as input the crystal information files (.cif) of the single-crystal structures. Differential scanning calorimetry was carried out on a Perkin–Elmer Diamond DSC instrument by heating and cooling the polycrystalline samples (9.8 mg) with a heating rate of 5 K/min in aluminum crucibles under nitrogen at atmospheric pressure. Variable-temperature second harmonic generation (SHG) experiments were executed by Kurtz-Perry powder SHG test using an unexpanded laser beam with low divergence (pulsed Nd:YAG at a wavelength of 1064 nm, 5 ns pulse duration, 1.6 MW peak power, 10 Hz repetition rate). The instrument model is Ins 1210058, INSTEC Instruments, while the laser is Vibrant 355 II, OPOTEK. The numerical values of the nonlinear optical coefficients for SHG have been determined by comparison with a KDP reference. The pressed-powder pellet sandwiched between two parallel copper electrodes was used for dielectric constant measurements. Complex dielectric permittivity ε ($\varepsilon = \varepsilon' - i\varepsilon''$) was measured on a Tonghui TH2828A instrument in the temperature range between 310 and 400 K with a frequency 1 MHz with an applied electric field of 1 V.

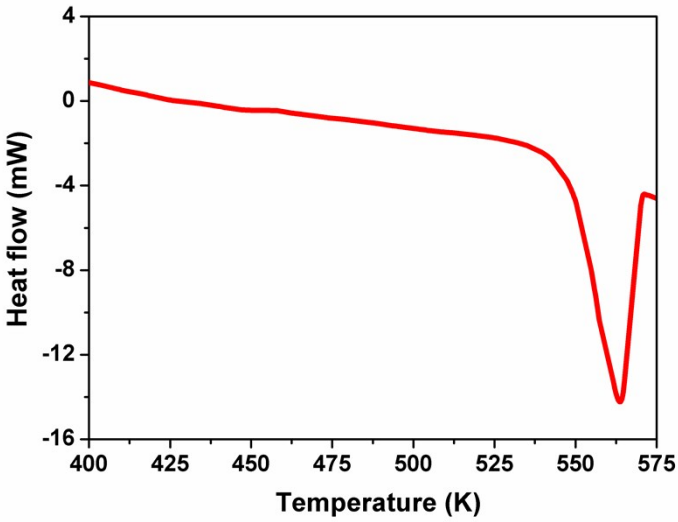

Fig. S1 DSC curves of **1** on heating, showing a melting endothermic peak around 563 K.

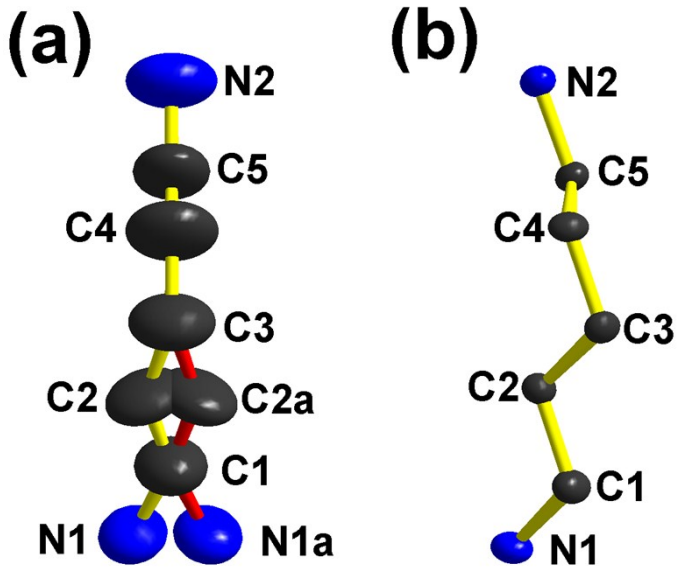

Fig. S2 1,5-pentanediammonium cation at (a) 393 and (b) 293 K. Thermal ellipsoids were shown at the 30% probability level. All hydrogen atoms were omitted for clarity.

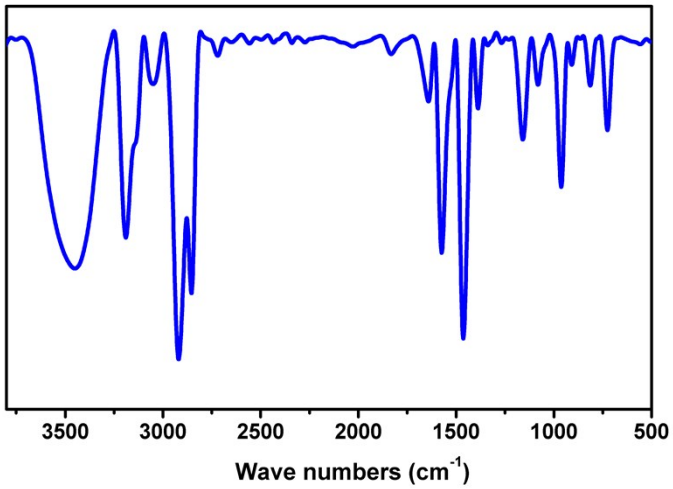

Fig. S3 Infrared (IR) spectra of solid **1** in KBr pellet recorded on a Shimadzu model IR-60 spectrometer at room temperature.

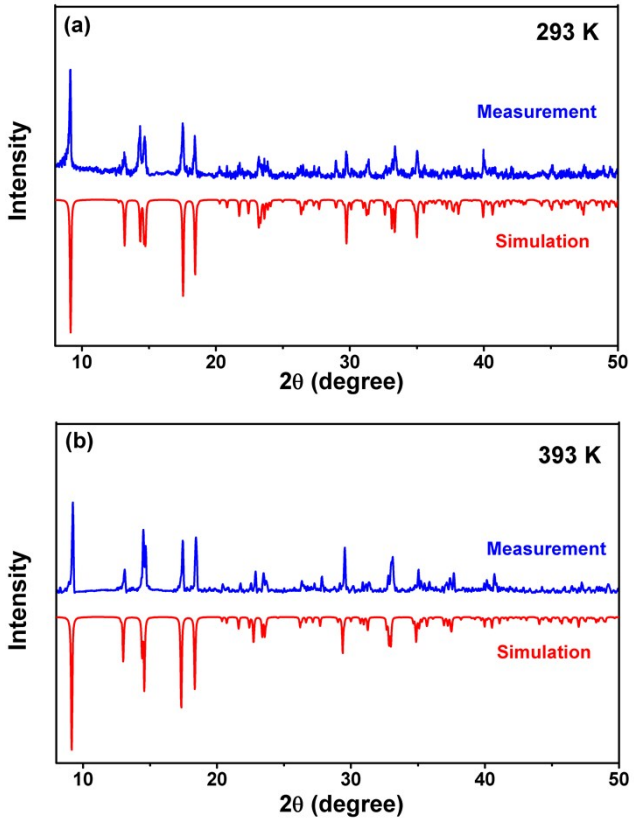

Fig. S4 X-ray powder diffraction (XRPD) of **1** at (a) 293 and (b) 393 K. The simulated powder diffraction patterns were calculated with the Mercury 3.1 program from the Cambridge Crystallographic Data Centre, using as input the crystal information files (.cif) of the single-crystal structures.

Table S1 Crystal data and structure refinements for **1** at 293 and 393 K.

Temperature	293 K	393 K
Empirical formula	$C_5H_{16}N_2$, $SbCl_5$	$C_5H_{16}N_2$, $SbCl_5$
Formula weight	403.21	403.21
Crystal system	orthorhombic	orthorhombic
Space group	$P2_12_12_1$	*Pnma*
a/Å	7.662(5)	13.514(10)
b/Å	13.433(9)	7.818(12)
c/Å	13.883(10)	13.80(2)
β/deg	90.00	90.00
Volume (Å^3), *Z*	1428.8(17), 4	1458(4), 4
Density (g cm^{-3})	1.874	1.837
*T*min/*T*max	0.397/0.479	0.405/0.486
F(000)	784	784
Reflections collected/unique	10417/3252	10124/1792
R_{int}	0.0466	0.0600
Parameters refined	121	83
Goodness-of-fit on F^2	1.003	1.037
R_1/wR_2 [$I>2\sigma(I)$]	0.0295/0.0507	0.0637/0.1308

Table S2. Selected bond lengths [Å] and angles [°] for **1**[a] at 293 and 393 K.

293 K	Sb1–Cl1	2.838(2)	Sb1–Cl1^{i}	2.977(2)

	Sb1–Cl2	2.615(2)	Sb1–Cl3	2.5049(8)
	Sb1–Cl4	2.685(8)	Sb1–Cl5	2.431(8)
	Cl1–Sb1–Cl1^{i}	86.1	Cl1–Sb1–Cl2	83.67(6)
	Cl1–Sb1–Cl4	89.93(6)	Cl1–Sb1–Cl5	88.30(7)
	Cl3–Sb1–Cl1^{i}	94.1	Cl3–Sb1–Cl2	94.43(7)
	Cl3–Sb1–Cl4	91.98(6)	Cl3–Sb1–Cl5	91.98(6)
	Cl2–Sb1–Cl1^{i}	88.9	Cl4–Sb1–Cl1^{i}	86.7
	Cl2–Sb1–Cl5	94.74(7)	Cl4–Sb1–Cl5	88.95(7)
393 K	Sb1–Cl1	2.874(3)	Sb1–Cl1^{ii}	2.874(3)
	Sb1–Cl2	2.687(4)	Sb1–Cl3	2.475(3)
	Sb1–Cl3^{iii}	2.475(3)	Sb1–Cl4	2.613(4)
	Cl1–Sb1–Cl1^{ii}	85.70(10)	Cl1–Sb1–Cl2	86.80(10)
	Cl1–Sb1–Cl3	90.82(11)	Cl1–Sb1–Cl4	87.78(9)
	Cl3^{iii}–Sb1–Cl1^{ii}	90.82(11)	Cl3^{iii}–Sb1–Cl2	95.96(11)
	Cl3^{iii}–Sb1–Cl3	92.50(15)	Cl3^{iii}–Sb1–Cl4	89.14(10)
	Cl2–Sb1–Cl1^{i}	86.80(10)	Cl4–Sb1–Cl1^{i}	87.78(9)
	Cl2–Sb1–Cl3	95.95(11)	Cl4–Sb1–Cl3	89.14(10)

[a]Symmetry codes:
(i) $x + 1/2, -y + 3/2, -z + 1$; (ii) $-x + 1, y - 1/2, -z + 1$; (iii) $x, -y + 3/2, z$.

Table S3. Geometrical parameters of the 1,5-pentanediammonium cation at 293 and 393 K.

293 K	N1–C1	1.471(6)	C1–C2	1.491(7)
	C2–C3	1.507(7)	C3–C4	1.527(7)
	C4–C5	1.503(7)	C5–N2	1.470(6)
	N1–C1–C2	113.2(5)	C1–C2–C3	112.2(5)
	C2–C3–C4	112.8(5)	C3–C4–C5	113.8(5)
	C4–C5–N2	111.3(4)		
	N1–C1–C2–C3	-178.9(5)	C1–C2–C3–C4	-178.5(5)
	C2–C3–C4–C5	-67.5(7)	C3–C4–C5–N2	179.4(5)
393 K	N1–C1	1.300(16)	C1–C2	1.225(19)

	C2–C3	1.288(19)	C3–C4	1.321(19)
	C4–C5	1.228(13)	C5–N2	1.313(12)
	N1–C1–C2	137.5(15)	C1–C2–C3	145(3)
	C2–C3–C4	142.9(17)	C3–C4–C5	138(2)
	C4–C5–N2	138.6(19)		
	N1–C1–C2–C3	-174(3)	C1–C2–C3–C4	112(3)
	C2–C3–C4–C5	-29(2)	C3–C4–C5–N2	180.0(4)

Table S4. Hydrogen-Bond Geometry (**Å**, deg) for the weak N–H···Cl at 293 and 393 K in **1**[b].

	D–H···A	H···A	D···A	D–H···A
293 K	N1–H1C···Cl2^{i}	2.41	3.299	172.5
	N1–H1D···Cl4^{ii}	2.72	3.279	121.6
	N1–H1E···Cl1^{iii}	2.53	3.372	157.9
	N2–H1C···Cl4^{iv}	2.39	3.272	170.3
	N2–H1D···Cl1	2.7	3.414	137.6
	N2–H1E···Cl3^{v}	2.57	3.403	155.3
393 K	N1–H1C···Cl4	2.66	3.318	131.1
	N1–H1D···Cl3^{vi}	2.49	3.343	159.2
	N1–H1E···Cl1	2.74	3.525	146.2
	N2–H1C···Cl2^{vii}	2.71	3.609	178.8
	N2–H1D···Cl3^{viii}	2.83	3.639	149.9
	N2–H1D···Cl1^{viii}	2.84	3.359	118.4

[b]Symmetry codes:
(i) $-x + 5/2, -y + 2, z + 1/2$; (ii) $-x + 2, y + 1/2, -z + 3/2$; (iii) $-x + 3/2, -y + 2, z + 1/2$; (iv) $x + 1/2, -y + 3/2, -z + 1$; (v) $x - 1/2, -y + 3/2, -z + 1$; (vi) $x - 1/2, y, -z + 1/2$; (vii) $x - 1/2, y, -z + 3/2$; (viii) $-x + 1/2, -y + 2, z + 1/2$.